Propagation of hybrid transverse magnetic-transverse electric plasmons on magnetically biased graphene sheets

J. S. Gómez-Díaz and J. Perruisseau-Carrier

Citation: Journal of Applied Physics **112**, 124906 (2012); doi: 10.1063/1.4769749
View online: http://dx.doi.org/10.1063/1.4769749
View Table of Contents: http://aip.scitation.org/toc/jap/112/12
Published by the American Institute of Physics

Propagation of hybrid transverse magnetic-transverse electric plasmons on magnetically biased graphene sheets

J. S. Gómez-Díaz[a] and J. Perruisseau-Carrier[a]
Adaptive MicroNanoWave Systems, LEMA/Nanolab, École Polytechnique Fédérale de Lausanne, 1015 Lausanne, Switzerland

(Received 28 August 2012; accepted 12 November 2012; published online 19 December 2012)

The propagation of plasmons on magnetically biased graphene sheets is addressed. The analysis is based on the transverse resonance method extended to handle the graphene conductivity tensor and allows easily accounting for substrate effects. A transcendental equation is obtained for the propagation constant of the resulting hybrid transverse magnetic-transverse electric mode. A closed-form approximate expression for a graphene layer sandwitched between two different media is also provided. Application of the method shows that the presence of a magnetic field leads to extreme field localization, namely, very small guided wavelength, as compared with usual plasmons in graphene or noble metals. The extent of field localization and its frequency can be dynamically controlled by modifying the applied magnetostatic and electrostatic bias field, respectively. These features could enable extreme device miniaturization and enhanced resolution in sensing applications. © *2012 American Institute of Physics*. [http://dx.doi.org/10.1063/1.4769749]

I. INTRODUCTION

Surface plasmons[1,2] are electromagnetic waves propagating along the interface between a conductor and a dielectric medium. They play a key role in the development of nanophotonics devices,[3] notably enabling the control of light at scales much smaller than the wavelength. So far they have mainly been studied using nobel metals, such as gold and silver, which provide well-confined surface plasmons in the visible range.[2] At terahertz and near infrared frequency bands, different configurations[4,5] have also been proposed to support plasmonic propagation. However, in all cases surface plasmons exhibit large losses at the desired operation frequency, which strongly limit potential applications.

The recent discovery of graphene[6] has provided an excellent alternative to support plasmon propagation[7] at terahertz and near infrared bands. In contrast with metal films, electrical and photonic properties of graphene can be controlled by means of external electrical and magnetic fields or chemical doping, leading to unprecedented phenomena and reconfigurability opportunities in the field of plasmonics.[8,31,32] The propagation of plasmons along monolayer graphene deposited on dielectric substrate has been studied by several authors both theoretically[7,9–11] and experimentally.[12] Generally speaking, graphene supports plasmons with enhanced field localization and similar losses at terahertz and near infrared as compared with those found in noble metals in the visible range.[7] It has also been shown that low temperature leads to an important reduction of plasmonic losses in graphene.[8] Recent studies have been focused on different graphene configurations to support plasmons, such as waveguides,[13] parallel graphene pairs,[9] or multilayered graphene stacks.[14,15] Recently, the presence of magnetoplasmons in large scale monolayer graphene was experimentally demonstrated.[16] However, the propagating features of these plasmons have not been yet considered.

Here, we investigate the characteristics of plasmons propagating on magnetically biased graphene sheets, taking into account substrate effects. Specifically, we consider the conductivity tensor obtained by applying an external magnetostatic bias to graphene[17] at terahertz. The dispersion relation of the propagating mode is obtained by applying the transverse resonance method,[18] extended to handle graphene tensorial conductivity, to a rigorous Green's function-based equivalent circuit.[19] In contrast with plasmons on magnetically unbiased graphene sheets,[10] the propagating plasmon is not a pure transverse magnetic (TM) mode but a hybrid transverse magnetic and transverse electric (TM-TE) mode. Some useful closed-form expressions for the propagation constant of surface waves on magnetically biased graphene sheets sandwiched between two media are provided. Results show that the presence of magnetostatic bias leads to unprecedent plasmon field localization, with extremely favorable values as compared with plasmons in magnetically unbiased graphene or in noble metals while preserving similar level of losses. In addition, it is shown that the adequate combination of electrostatic and magnetostatic biasing fields provides an excellent control of plasmonic properties, including the extent of field localization enhancement and its location in frequency. All these features make plasmons propagating on magnetically biased graphene sheets ideal candidates for extreme miniaturized devices, sensing applications,[20] and to devise non-linear devices.[21]

The paper is organized as follows. Section II describes a Green's function-based equivalent circuit to rigorously characterize magnetically biased graphene, providing analytical relations between the equivalent admittances of the circuit and the components of the graphene conductivity tensor. Then, in Sec. III we derive the dispersion relation of hybrid TM-TE plasmons and provide closed-form approximations for some practical cases. Section IV discusses the characteristics of plasmons on magnetically biased graphene sheets, including slow-wave factor, losses, and z-decay rate. Finally, Section V concludes the paper.

[a]Electronic mail: juan-sebastian.gomez@epfl.ch, julien.perruisseau-carrier@epfl.ch

II. RIGOROUS EQUIVALENT CIRCUIT OF A MAGNETICALLY BIASED GRAPHENE SHEET

Let us consider a graphene sheet in the plane $z=0$ and separating two media, as shown in Fig. 1(a). Graphene is described using a tensorial conductivity $\bar{\bar{\sigma}}$[11,17]

$$\bar{\bar{\sigma}}(\omega,\mu_c(\vec{E}_0),\Gamma,T,\vec{B}_0)=\begin{pmatrix}\sigma_{xx} & \sigma_{xy}\\ \sigma_{yx} & \sigma_{yy}\end{pmatrix}=\begin{pmatrix}\sigma_d & \sigma_0\\ -\sigma_0 & \sigma_d\end{pmatrix}, \quad (1)$$

where ω is the angular frequency, μ_c is the chemical potential (which depends on the chemical doping and on the applied electrostatic bias field, $\vec{E}_0=E_0\hat{e}_z$), T is temperature, Γ is the phenomenological electron scattering rate, and $\vec{B}_0=B_0\hat{e}_z$ is the applied magnetostatic bias field. In addition, σ_d and σ_0 are the direct and Hall conductivity of graphene. These conductivities can be obtained from Kubo's formalism as[17,22]

$$\sigma_d(\mu_c(E_0),B_0)=\frac{q_e^2v_f^2|q_eB_0|(\omega-j2\Gamma)\hbar}{-j\pi}\times\sum_{n=0}^{\infty}\left\{\frac{f_d(M_n)-f_d(M_{n+1})+f_d(-M_{n+1})-f_d(-M_n)}{(M_{n+1}-M_n)^2-(\omega-j2\Gamma)^2\hbar^2}\times\left(1-\frac{\Delta^2}{M_nM_{n+1}}\right)\right.$$
$$\left.\times\frac{1}{M_{n+1}-M_n}+\frac{f_d(-M_n)-f_d(M_{n+1})+f_d(-M_{n+1})-f_d(M_n)}{(M_{n+1}+M_n)^2-(\omega-j2\Gamma)^2\hbar^2}\times\left(1+\frac{\Delta^2}{M_nM_{n+1}}\right)\frac{1}{M_{n+1}+M_n}\right\}, \quad (2)$$

$$\sigma_0(\mu_c(E_0),B_0)=-\frac{q_e^2v_f^2q_eB_0}{\pi}\sum_{n=0}^{\infty}\{f_d(M_n)-f_d(M_{n+1})-f_d(-M_{n+1})+f_d(-M_n)\}$$
$$\times\left\{\left(1-\frac{\Delta^2}{M_nM_{n+1}}\right)\frac{1}{(M_{n+1}-M_n)^2-(\omega-j2\Gamma)^2\hbar^2}+\left(1+\frac{\Delta^2}{M_nM_{n+1}}\right)\frac{1}{(M_{n+1}+M_n)^2-(\omega-j2\Gamma)^2\hbar^2}\right\}, \quad (3)$$

where

$$f_d(M_n)=\frac{1}{1+e^{(M_n-\mu_c)/k_BT}} \quad (4)$$

is the Fermi-Dirac distribution, M_n is defined as

$$M_n=\sqrt{\Delta^2+2nv_f^2|q_eB_0|\hbar}, \quad (5)$$

$\hbar$ is the reduced Planck constant, $-q_e$ is the charge of an electron, v_F is the electron velocity in graphene (which is considered $\approx 10^6$ m/s and independent of energy), and Δ is an excitonic energy gap, which is usually negligible at room temperatures.[11,23] This model, which considers intraband and interband contributions of graphene conductivity and assumes a constant scattering rate for the whole frequency range, has been validated using measured data.[17] It is worth mentioning that this model does not take spatial dispersion[11,24] into account (conductivity does not depend on the propagation constant of the plasmon) and that it has been derived for an isolated graphene sheet. Specifically, spatial dispersion may affect the characteristics of plasmons propagating on graphene, including sheets[7] or nonhomogeneous double layer structures.[25] In the particular case of magnetically unbiased graphene sheets, it is known that spatial dispersion increases losses and slightly reduces the mode confinement of the propagating plasmons at high frequencies.[7] However, in the frequency range considered here (1 – 50 THz) these effects are small, and the approximate graphene model described above[17] still provides an accurate characterization of the plasmons propagating on the structure.

The electromagnetic interaction of the graphene sheet with the surrounding dielectrics is rigorously modeled by an equivalent transmission line model,[19] as shown in Fig. 1(b).

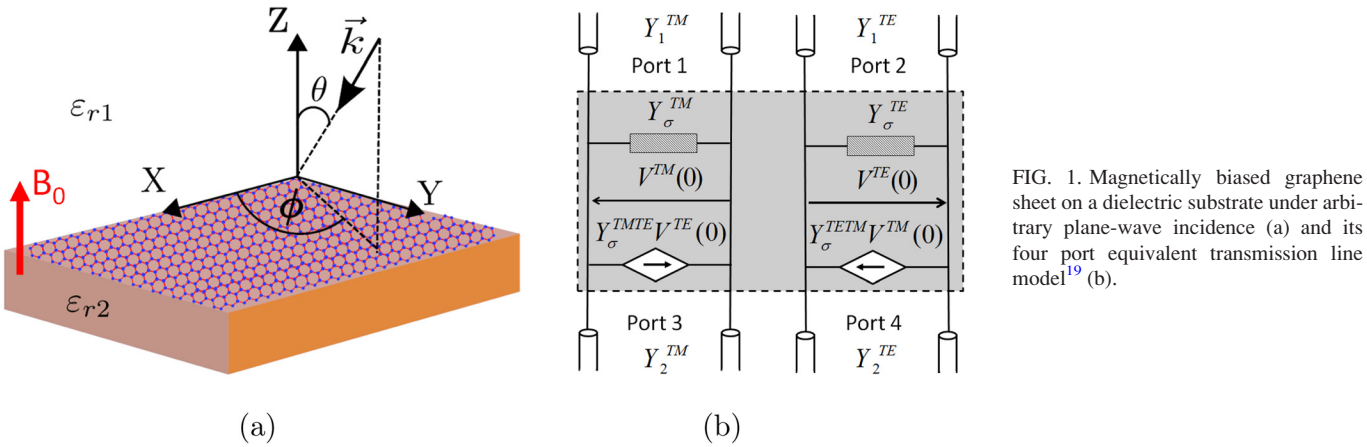

FIG. 1. Magnetically biased graphene sheet on a dielectric substrate under arbitrary plane-wave incidence (a) and its four port equivalent transmission line model[19] (b).

In order to derive this circuit model, a uniform plane wave impinging onto the graphene sheet from the upper half space ($z > 0$), as illustrated in Fig. 1(a), is considered. The incident wave has a wavenumber $\vec{k} = k_x\hat{e}_x + k_y\hat{e}_y + k_z\hat{e}_z$, where $k_x = k_1\cos(\phi)\sin(\theta)$, $k_y = k_1\sin(\phi)\sin(\theta)$, $k_z = k_1\cos(\theta)$, and $k_1 = \sqrt{\varepsilon_{r1}\mu_{r1}}k_0$ is the wavenumber of medium 1. Then, the usual analogy between plane wave propagation in stratified media and the currents and voltages along an uniform transmission line is applied.[26] Using this approach, boundary conditions are imposed on the graphene sheet,[19] rigorously leading to the equivalent circuit shown in Fig. 1(b). This circuit is a four-port network where ports 1 and 3 relates input and output TM waves through the shunt admittance Y_σ^{TM}, ports 2 and 4 relates input and output TE waves through the shunt admittance Y_σ^{TE}, and the cross-coupling between the two polarizations is accurately taken into account by voltage-controlled current generators, with coefficients $Y_\sigma^{TE/TM}$ and $Y_\sigma^{TM/TE}$ for TE-TM and TM-TE coupling, respectively. The relationship between the components of graphene conductivity and the admittances of the equivalent circuit is analytically obtained as[19]

$$Y_\sigma^{TE} = Y_\sigma^{TM} = \sigma_d, \quad Y_\sigma^{TE/TM} = -Y_\sigma^{TM/TE} = \sigma_0. \tag{6}$$

III. DISPERSION RELATION FOR HYBRID TM-TE PLASMONS

The availability of analytical expressions for the equivalent admittances of graphene allows to compute the dispersion relation of a magnetically biased graphene sheet sandwiched between two media (see Fig. 1(a)), which is obtained by imposing a transverse resonance equation[18] (TRE) to the equivalent transmission line circuit of the structure shown in Fig. 1(b). The solution of this equation provides the propagation constant of the plasmons propagating on the graphene sheet. The TRE is a well-known technique in electromagnetics[18] which allows to compute dispersion relations of complicated structures, such as dielectric-loaded waveguides[27] or leaky-wave antennas[28] and resonance frequencies of cavities.[27]

In order to impose the TRE to the structure shown in Fig. 1(a), the four port equivalent network of Fig. 1(b) is transformed into a more convenient—yet rigorously equivalent—circuit. For this purpose, we first load the different ports of the transmission line model with the TM and TE characteristics admittances of their corresponding media, leading to the simplified circuit shown in Fig. 2(a). These characteristics admittances are defined as

$$\begin{aligned} Y_1^{TE} &= \frac{k_{z_1}}{\omega\mu_{r_1}\mu_0}, \quad Y_2^{TE} = \frac{k_{z_2}}{\omega\mu_{r_2}\mu_0}, \\ Y_1^{TM} &= \frac{\omega\varepsilon_{r_1}\varepsilon_0}{k_{z_1}}, \quad Y_2^{TM} = \frac{\omega\varepsilon_{r_2}\varepsilon_0}{k_{z_2}}, \end{aligned} \tag{7}$$

where $k_{z_1} = \pm\sqrt{k_1^2 - k_\rho^2}$ and $k_{z_2} = \pm\sqrt{k_2^2 - k_\rho^2}$ are the transverse ("z" direction) wavenumbers of medium 1 and 2, $k_1 = \sqrt{\varepsilon_{r_1}\mu_{r_1}}k_0$ and $k_2 = \sqrt{\varepsilon_{r_2}\mu_{r_2}}k_0$ are the intrinsic wavenumbers of medium 1 and 2, and k_ρ is the complex propagation constant of the surfaces waves propagating on the graphene sheet. Then, we apply simple circuit theory to remove the voltage-controlled current sources which couples the TM and TE modes, leading to a single circuit with combined TM-TE characteristics. Specifically, we focus on the TE branch of the equivalent circuit of Fig. 2(a) (a completely similar development can easily be done starting from the TM branch) and combine its admittances, leading to the simplified circuit depicted in Fig. 2(b). Next, the voltage on the TE branch of the circuit [denoted as $V^{TE}(0)$ in the right circuit of Fig. 2(b)] is computed using

$$V^{TE}(0) = \frac{Y_\sigma^{TM/TE}}{Y_1^{TE} + Y_2^{TE} + Y_\sigma^{TE}}. \tag{8}$$

Using the above definition of $V^{TE}(0)$, the voltage-dependent TM current generator (see the left circuit of Fig. 2(b)) can easily be substituted by a simple admittance Y^C, defined as

$$Y^C = \frac{Y_\sigma^{TM/TE}Y_\sigma^{TE/TM}}{Y_1^{TE} + Y_2^{TE} + Y_\sigma^{TE}}, \tag{9}$$

and where the TE "effect" of the circuit has been absorbed. This simple procedure allows to transform the original four port transmission line model of Fig. 1(b) into the simplified yet rigorous equivalent circuit shown in Fig. 2(c).

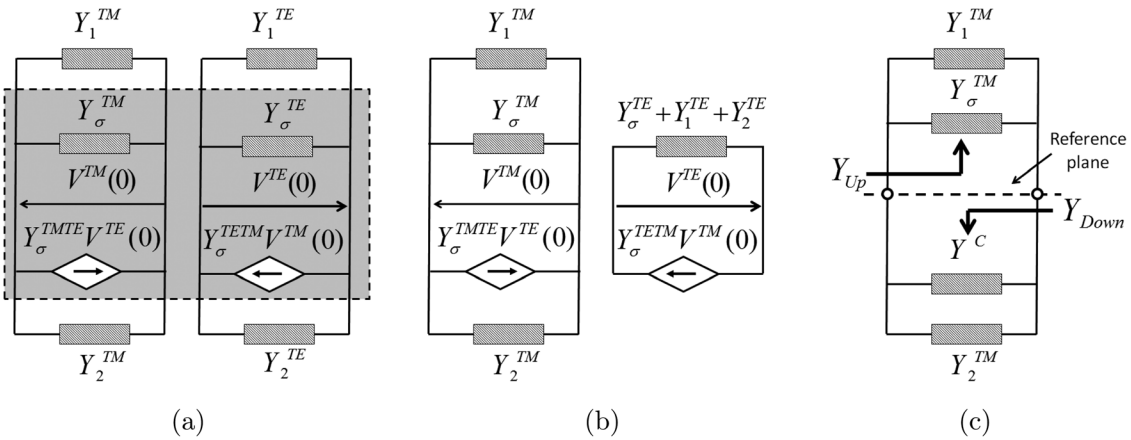

FIG. 2. Equivalent circuit models of a magnetically biased graphene sheet sandwiched between two media (see Fig. 1).

Then, the TRE[18] formalism is applied to this equivalent circuit, setting the reference plane of the TRE at the graphene sheet (see Fig. 2(c)). This allows to obtain the propagating constant of the surface waves propagating on the graphene sheet. The TRE also requires to compute the input impedances observed from the reference plane. These impedances are denoted as Y_{Up} and Y_{Down} (see Fig. 2(c)) and are obtained as

$$\begin{aligned} Y_{Up} &= Y_1^{TM} + Y_\sigma^{TM}, \\ Y_{Down} &= Y_2^{TM} + Y^C = Y_2^{TM} + \frac{Y_\sigma^{TM/TE} Y_\sigma^{TE/TM}}{Y_1^{TE} + Y_2^{TE} + Y_\sigma^{TE}}. \end{aligned} \tag{10}$$

Finally, the TRE is imposed at the reference plane of the circuit, leading to the equation $Y_{Up} + Y_{Down} = 0$. After straightforward manipulations, this expression can be simplified as

$$\begin{aligned} &(Y_1^{TE} + Y_2^{TE} + Y_\sigma^{TE})(Y_1^{TM} + Y_2^{TM} + Y_\sigma^{TM}) \\ &\quad + Y_\sigma^{TE/TM} Y_\sigma^{TM/TE} = 0, \end{aligned} \tag{11}$$

and substituting the equivalent admittances by their values

$$\begin{aligned} &\left(\frac{\pm\sqrt{k_1^2 - k_\rho^2}}{\omega\mu_{r_1}\mu_0} + \frac{\pm\sqrt{k_2^2 - k_\rho^2}}{\omega\mu_{r_2}\mu_0} + \sigma_d \right) \\ &\quad \times \left(\frac{\omega\varepsilon_{r_1}\varepsilon_0}{\pm\sqrt{k_1^2 - k_\rho^2}} + \frac{\omega\varepsilon_{r_2}\varepsilon_0}{\pm\sqrt{k_2^2 - k_\rho^2}} + \sigma_d \right) = \sigma_0^2. \end{aligned} \tag{12}$$

This equation provides the dispersion relation of a magnetically biased graphene sheet, including substrate effects. It should be noted that in contrast with the case of pure TM plasmonic mode propagating on magnetically unbiased graphene,[7] the solution of this equation leads to the propagation constant (k_ρ) of a hybrid TM-TE mode. Note that the hybrid mode arises due to the presence of a magnetostatic biasing field, which provides the coupling between the TM and TE modes. It is also worth mentioning that Eq. (12) does not admit analytical solution and must be solved employing numerical methods such as the Newton-Raphson algorithm.[29] However approximate analytical solutions of Eq. (12) can be found as a function of the parameters of surrounding media, as discussed below.

A. Graphene sheet in an homogeneous media

We consider here a graphene sheet surrounded by an homogeneous medium, i.e., the dielectrics above and below the graphene sheet are the same. The characteristics of this medium are defined as $\varepsilon_r = \varepsilon_{r_1} = \varepsilon_{r_2}$, $\mu_r = \mu_{r_1} = \mu_{r_2}$, and $k = k_1 = k_2$. In this case, the exact solution of Eq. (12) yields[11]

$$k_\rho = k\sqrt{\frac{-(1 + s_d^4 - 2s_d^2)^2 - b \pm \sqrt{(s_d^4 + b - 1)^2 + 4b}}{2s_d^2}}, \tag{13}$$

where

$$\begin{aligned} &s_d = \frac{\eta\sigma_d}{2}, \quad s_0 = \frac{\eta\sigma_0}{2}, \quad \eta = \sqrt{\frac{\mu_0\mu_r}{\varepsilon_0\varepsilon_r}}, \quad \text{and} \\ &b = s_0^2[s_0^2 + 2(1 + s_d^2)]. \end{aligned} \tag{14}$$

Note that in the absence of a magnetostatic biasing field ($Y_\sigma^{TE/TM} = Y_\sigma^{TM/TE} = \sigma_0 = s_0 = 0$), Eq. (13) reduces to well-known expressions for decoupled TM and TE propagating modes.[10]

B. Graphene sheet sandwiched between two different media

We consider here a graphene sheet sandwiched between two different non-magnetic media ($\mu_{r_1} = \mu_{r_2} = 1$), as shown in Fig. 1(a). In the usual non-retarded regime[7] ($k_\rho \gg k_0$), where plasmons propagates, Eq. (13) can be solved as

$$\begin{aligned} k_\rho \approx{}& \frac{jk_0}{2}\left[\frac{\varepsilon_{r_1} + \varepsilon_{r_2}}{\eta_0\sigma_d} + \frac{\eta_0}{2\sigma_d}(\sigma_d^2 + \sigma_0^2)\right] \\ &+ \frac{jk_0}{2}\sqrt{\left[\frac{\varepsilon_{r_1} + \varepsilon_{r_2}}{\eta_0\sigma_d} + \frac{\eta_0}{2\sigma_d}(\sigma_d^2 + \sigma_0^2)\right]^2 - 2(\varepsilon_{r_1} + \varepsilon_{r_2})}. \end{aligned} \tag{15}$$

As in the previous case, in the absence of a magnetostatic biasing field ($Y_\sigma^{TE/TM} = -Y_\sigma^{TM/TE} = \sigma_0 = 0$) this equation reduces to a well-known expression for TM plasmons.[7]

IV. PROPERTIES OF HYBRID TM-TE PLASMONS

In this section, we investigate the characteristics of plasmons propagating on magnetically biased graphene, taking substrate influences into account. Specifically, we focus on properties such as field localization or slow wave factor, defined as ($Re[k_\rho/k_0]$), losses ($Re[k_\rho]/Im[k_\rho]$), and z-decay rate $\left(L_{z_0} = \frac{1}{|\mathrm{Im}(k_{z_1})|}\right)$ and compare them with the usual features of plasmonic waves propagating on magnetically unbiased graphene.[7] In our study, we consider $T = 300$ K (room temperature) and a relaxation time of 0.135 ps, in agreement with measured values of graphene carrier mobility.[6,7] For the sake of simplicity, we neglect the possible frequency variation of the relaxation time due to optical phonons.[7]

Here we examine plasmonic characteristics as a function of an external magnetostatic bias field, neglecting the influence of spatial dispersion.[11] First, we consider the simple case of a graphene sheet, with chemical potential $\mu_c = 0$ eV, surrounded by air. Fig. 3(a) shows the variations of the direct graphene conductivity σ_d (related to the equivalent admittances Y_σ^{TM} and Y_σ^{TE}, see Sec. II) as a function of the applied magnetostatic bias. The slow-wave factor related to a plasmon wave propagating on this graphene sheet is shown in Fig. 3(b). The hybrid TM-TE mode exhibits excellent plasmonic features (TM-like plasmon mode[7]) or extremely weak mode confinement (TE-like plasmon mode[7]), as a function of the sign of $Im[\sigma_d]$ [see Eq. (13)]. When $Im[\sigma_d] > 0$, large field localization is obtained versus the applied magnetic field while preserving similar loss as in the case of magnetically unbiased graphene. Note that this excellent field

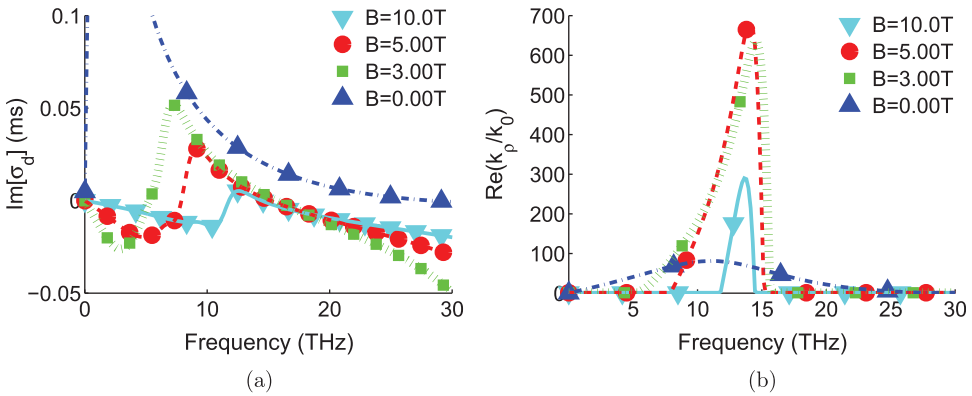

FIG. 3. Influence of applied magnetostatic biasing field in the direct conductivity of graphene[30] (a) and in the slow-wave factor a plasmonic wave propagating on a graphene sheet surrounded by air (b). Graphene parameters are $\tau = 0.135$ ps, $\mu_c = 0$ eV, and $T = 300$ K.

localization does not only depend on σ_d but also on the Hall conductivity σ_0. Besides, the applied magnetostatic bias not only allows controlling the characteristics of the propagating plasmons but also its location in frequency. When $Im[\sigma_d] < 0$, the hybrid TM-TE mode presents poor plasmon characteristics ($k_\rho \approx k_0$).

Consider now the more realistic case of a graphene sheet, with chemical potential $\mu_c = 0.1$ eV, deposited on a dielectric substrate, with $\varepsilon_r = 11.9$. Fig. 4 shows the characteristics of a plasmon wave propagating on the sheet, including slow-wave factor, losses, and z-decay rate, as a function of the applied magnetostatic field. Note that, in contrast with the previous case, the hybrid TM-TE mode only exists in a certain frequency range (where $Im[\sigma_d] > 0$). This is because this mode is not supported if $Im[\sigma_d] < 0$ and the graphene sheet is sandwiched between two different media, as can be demonstrated from Eq. (12). It is also worth mentioning that the finite chemical potential up-shifts the frequency range where the influence of magnetic bias is appreciable. Results show extreme field localization versus the applied magnetostatic field, with peak values of $Re[k_\rho/k_0] \approx 7000$ at around 37 THz. For comparison, note that a plasmon propagating on a magnetically unbiased graphene sheet, with similar intrinsic characteristics, has a maximum of 940 and that a plasmon along an Ag/Si interface, around 20. In addition, other plasmon characteristics, such as losses factor and z-decay rate, presents similar values as in the case of magnetically unbiased graphene.

Finally, we present in Fig. 5 the characteristics of a plasmon propagating on a similar environment, but for the higher chemical potential of $\mu_c = 0.25$ eV. It can be seen that the influence of the magnetostatic bias here is limited. This is due to the large value of chemical potential, which up-shifts the frequency range where the influence of magnetostatic bias is significant. Consequently, large chemical potentials dominate over magnetostatic bias on the plasmon response at

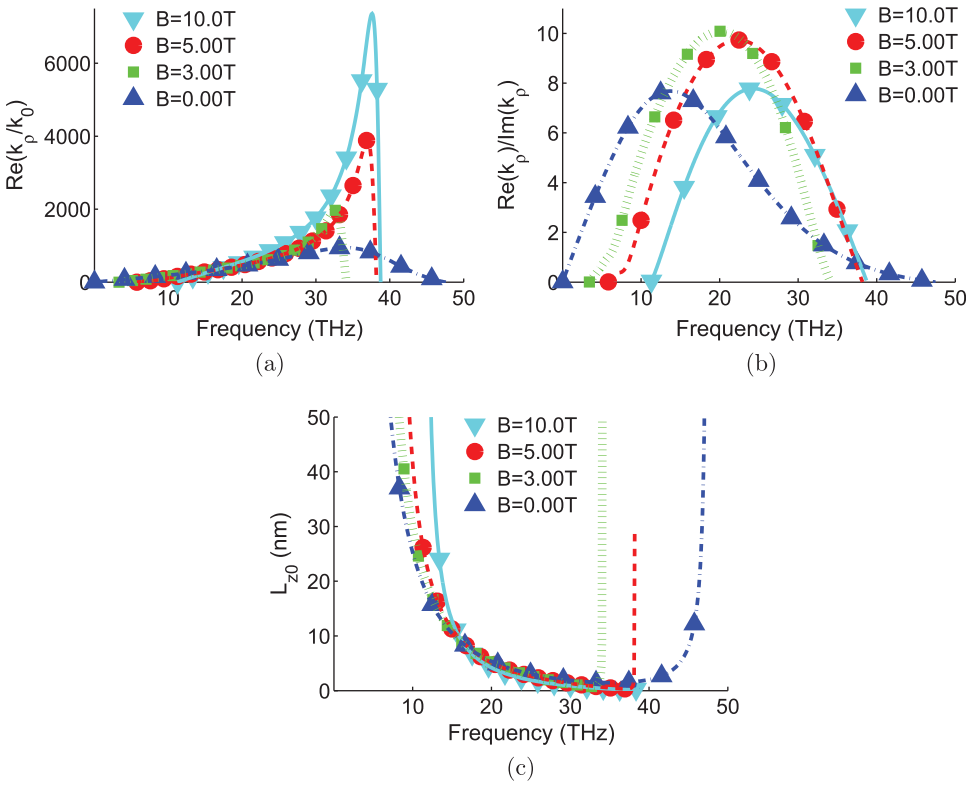

FIG. 4. Slow-wave factor (a), losses (b), and z-decay rate (c) of a plasmonic wave propagating on an air-graphene-dielectric interface versus applied magnetostatic bias field. The dielectric permittivity is $\varepsilon_r = 11.9$ and graphene parameters are $\tau = 0.135$ ps, $\mu_c = 0.1$ eV, and $T = 300$ K.

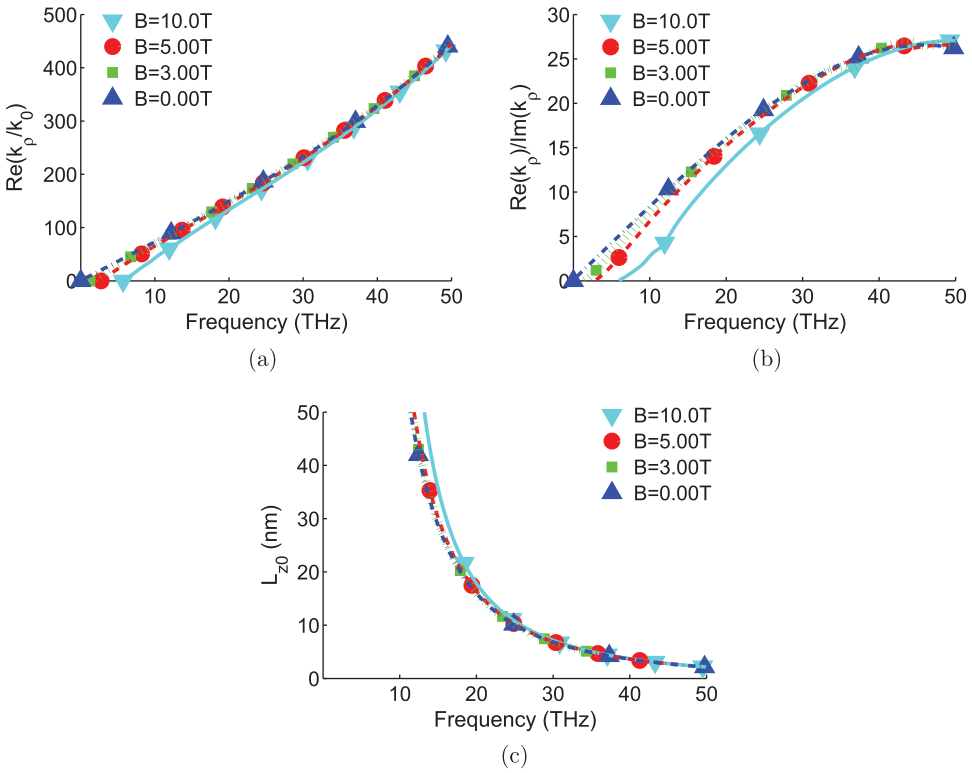

FIG. 5. Slow-wave factor (a), losses (b), and z-decay rate (c) of a plasmonic wave propagating on an air-graphene-dielectric interface versus applied magnetostatic bias field. The dielectric permittivity is $\varepsilon_r = 11.9$ and graphene parameters are $\tau = 0.135$ ps, $\mu_c = 0.25$ eV, and $T = 300$ K.

terahertz and near infrared bands. As expected, the increase of the chemical potential reduces losses with respect to the previous example.

It should be noted that an adequate combination of external electrostatic and magnetostatic biasing fields provides a great capability to control plasmonic properties. Indeed, the variation of the electrostatic bias field, which modifies the chemical potential μ_c, controls the desired frequency region and reduce losses, while the magnetostatic bias field allows affecting the extent of field localization (see Figs. 3(b), 4, and 5).

V. CONCLUSIONS AND OUTLOOK

The propagation of plasmons on magnetically biased graphene sheets, taking substrate effects into account, has been addressed. The tensorial conductivity of graphene, which arises due to the presence of an external magnetostatic bias field, was considered in the terahertz region. The proposed analysis was based on the transverse resonance method extended to handle graphene tensorial conductivity, leading to the desired dispersion relation. In contrast with magnetically unbiased graphene, plasmons are not anymore completely pure TM modes but hybrid TM-TE ones. Closed-formed approximate expressions for the propagation constant of plasmons on graphene sheets sandwiched by two different media were also been provided.

Our results have shown that plasmons propagating on magnetically biased graphene present a dramatic field localization, while preserving similar characteristics in terms of losses and z-decay rate. Also, the extent of field localization and its frequency can externally be tuned by modifying the applied magnetostatic and electrostatic biasing field, respectively. For example, we can see in Fig. 4(a) that extremely high field localization ($Re[k_\rho/k_0] \approx 7000$) is possible, substantially higher than in conventional surface plasmons (for example, $Re[k_\rho/k_0] \approx 900$ and $Re[k_\rho/k_0] \approx 20$ in a similar magnetically unbiased graphene and in an Ag/Si interface, respectively). This interesting feature can be used in sensing applications,[20] to devise non-linear components[21] and to achieve extreme device miniaturization.

ACKNOWLEDGMENTS

This work was supported by the Swiss National Science Foundation (SNSF) under grant 133583 and by the EU FP7 Marie-Curie IEF grant "Marconi," with Ref. 300966. The authors wish to thank Dr. Garcia-Vigueras (UPCT, Spain) for fruitful discussions.

[1]J. M. Pitarke, V. M. Silkin, E. V. Chulkov, and P. M. Echenique, "Theory of surface plasmons and surface-plasmon polaritons," Rep. Prog. Phys. **70**, 1–87 (2007).
[2]Y. Wang, E. W. Plummer, and K. Kempa, "Foundations of plasmonics," Adv. Phys. **60**, 799–898 (2011).
[3]W. L. Barnes, A. Dereux, and T. W. Ebbesen, "Surface plasmon subwavelength optics," Nature (London) **424**, 824–830 (2003).
[4]J. B. Pendry, L. Martín-Moreno, and F. J. Garcia-Vidal, "Mimicking surface plasmons with structured surfaces," Science **305**, 847–848 (2004).
[5]J. Elser, A. A. Govyadinov, I. Avrutsky, I. Salakhutdinov, and V. A. Podolskiy, "Plasmonic nanolayer composites: Coupled plasmon polaritons, effective-medium response, and subdiffraction light manipulation," J. Nanomater. **2007**, 79469.
[6]K. S. Novoselov, A. K. Geim, S. V. Morozov, D. Jiang, Y. Zhang, S. V. Dubonos, I. V. Grigorieva, and A. A. Firsov, "Electric field effect in atomically thin carbo filts," Science **306**, 666–669 (2004).
[7]M. Jablan, H. Buljan, and M. Soljacic, "Plasmonics in graphene at infrared frequencies," Phys. Rev. B **80**, 245435 (2009).
[8]A. Vakil and N. Engheta, "Transformation optics using graphene," Science **332**, 1291–1294 (2011).
[9]E. H. Hwang and J. D. Sarma, "Dielectric function, screening, and plasmons in two-dimensional graphene," Phys. Rev. B **75**, 205418 (2007).

[10]G. W. Hanson, "Dyadic green's functions and guided surface waves for a surface conductivity of graphene," J. Appl. Phys. **103**, 064302 (2008).
[11]G. W. Hanson, "Dyadic green's functions for an anisotropic non-local model of biased graphene," IEEE Trans. Antennas Propag. **56**, 747–757 (2008).
[12]J. T. Kim and S. Y. Choi, "Graphene-based plasmonic waveguides for photonic integrated circuits," Opt. Express **19**, 24557 (2011).
[13]J. Christensen, A. Manjavacas, S. Thongrattanasiri, F. H. L. Koppens, and F. J. G. de Abajo, "Graphene plasmon waveguiding and hybridization in individual and paired nanoribbons," ACS Nano **6**, 431–440 (2012).
[14]L. A. Falkovsky and S. S. Pershoguba, "Optical far-infrared properties of a graphene monolayer and multilayer," Phys. Rev. B **76**, 153410 (2007).
[15]C. H. Gan, H. S. Chu, and E. P. Li, "Synthesis of highly-confined surface plasmon modes with doped graphene sheets in the mid-infrared and terahertz frequencies," Phys. Rev. B **85**, 125431 (2012).
[16]I. Crasse, M. Orlita, M. Potemski, A. L. Walter, M. Ostler, T. Seyller, I. Gaponenko, J. Chen, and A. B. Kuzmenko, "Intrinsic terahertz plasmons and magnetoplasmons in large scale monolayer graphene," Nano Lett. **12**, 2470–2474 (2012).
[17]V. P. Gusynin, S. G. Sharapov, and J. P. Carbotte, "Magneto-optical conductivity in graphene," J. Phys.: Condens. Matter **19**(2), 026222 (2007).
[18]R. E. Collin and F. J. Zucker, *Antenna Theory* (McGraw-Hill, 1969).
[19]G. Lovat, "Equivalent circuit for electromagnetic interaction and transmission through graphene sheets," IEEE Trans. Electromagn. Compat. **54**, 101–109 (2012).
[20]M. E. Stewart, C. R. Anderton, L. B. Thompson, J. Maria, S. K. Gray, J. A. Rogers, and R. G. Nuzzo, "Nanostructured plasmonic sensors," Chem. Rev. **108**, 494–521 (2008).
[21]M. Soljacic and J. D. Joannopoulos, "Enhancement of nonlinear effects using photonic crystals," Nat. Mater. **3**, 211 (2004).
[22]M. Dressel and G. Gruner, *Electrodynamics of Solids* (Cambridge University Press, Cambridge, UK, 2002).
[23]E. V. Gorbar, V. P. Gusynin, V. A. Miransky, and I. A. Shovkovy, "Magnetic field driven metal-insulator phase transition in planar systems," Phys. Rev. B **66**, 045108 (2002).
[24]L. A. Falkovsky and A. A. Varlamov, "Space-time dispersion of graphene conductivity," Eur. Phys. J. B **56**, 281–284 (2007).
[25]S. M. Badalyan and F. M. Peeters, "Effect of nonhomogeneous dielectric background on the plasmon modes in graphene double-layer structures at finite temperatures," Phys. Rev. B **85**, 195444 (2012).
[26]K. A. Michalski and J. R. Mosig, "Multilayered media Green's functions in integral equation formulations," IEEE Trans. Antennas Propag. **45**, 508–519 (1997).
[27]D. Pozar, *Microwave Engineering*, 3rd ed. (John Wiley & Sons, 2005).
[28]A. A. Oliner and D. R. Jackson, "Leaky-wave antennas," in *Antenna Engineering Handbook*, edited by J. L. Volakis, 4th ed. (McGraw-Hill, New York, 2007).
[29]W. H. Press, S. A. Teukolsky, W. T. Vetterling, and B. P. Flannery, *Numerical Recipes in Fortran 90, The Art of Parallel Scientific Computing* (Cambridge University Press, 1996).
[30]V. P. Gusynin, S. G. Sharapov, and J. B. Carbotte, "On the universal ac optical background in graphene," New J. Phys. **11**, 095013 (2009).
[31]M. Tamagnone, J. S. Gomez-Diaz, J. R. Mosig, and J. Perruisseau-Carrier, "Reconfigurable THz Plasmonic Antenna Concept Using a Graphene Stack," Appl. Phys. Lett. **101**, 214102 (2012).
[32]N. M. R. Peres, A. Ferreira, Y. V. Bludov, and M. I. Vasilevskiy, "Light scattering by a medium with aspatially modulated optical conductivity: the case of graphene," J. Phys.: Condens. Matter **24**, 245303 (2012).